J|A|C|S
ARTICLES
Published on Web 03/30/2007

Self-Duplex Formation of an A^{Py}-Substituted Oligodeoxyadenylate and Its Unique Fluorescence

Young Jun Seo, Hanju Rhee, Taiha Joo, and Byeang Hyean Kim*

Contribution from the Department of Chemistry, BK School of Molecular Science, Pohang University of Science and Technology, Pohang 790-784, Korea

Received December 18, 2006; E-mail: bhkim@postech.ac.kr

Abstract: Unexpected homoadenine self-duplexes are formed when pyrene units are bound covalently to the deoxyadenosine bases at specific distances (1,4 relationships). This discovery illustrates how small-molecule pyrene intercalators can be used to drive unknown nucleic acid assembly with a concomitant change in fluorescence. When a pair of pyrene fluorophore units is located within an oligodeoxyadenylate chain, the system can display three different colors (reddish-orange, green, or blue) depending on the relative location of the fluorophores. A unique fluorescence signal, a reddish band peaking at 580 nm, appears when the oligomers possess more than two spacers between the pyrene fluorophores(1,4 relationships). Several spectroscopic experiments, for example, recording variable-concentration spectra, CD, UV, melting temperature, and gel electropherogram, indicate that this new reddish band came from an intermolecular homoadenine self-duplex. Time-resolved fluorescence measurements using both TCSPC and upconversion methods indicate that this unique fluorescence has a long lifetime.

Introduction

π-Stacking interactions between base-pairs and sequences of nucleotides are the major interactions that stabilize DNA double helices; these interactions play a critical role in affecting the conformational diversity of DNA, which is essential for biological processes to occur in cells.[1] Intercalators, which are generally nonpolar, hydrophobic, planar molecules, are representative stacking materials that induce the formation of stable duplex DNA.[2] We are interested in using intercalators in a general manner to drive the assembly of nucleic acids and to effect structural transitions. Although there have been many studies of hydrophobic stacking interactions between small-molecule intercalators and duplex DNA,[3] we report the first example of a covalently linked intercalator inducing the formation of a self-duplex (homo adenine duplex) of DNA. We used oligodeoxyadenylates as templates because we hoped that their rigid conformations—resulting from their proclivity to form strong base stacks, even in single strands,[4]—would result in their ready stacking to form secondary structures. For the covalently bound intercalator, we used the pyrene derivative $\mathbf{A^{Py}}$, because pyrene is a fluorophore that possesses a highly nonpolar, planar structure and exhibits excellent $\pi-\pi$ stacking ability.[5]

Results and Discussion

The modified nucleotide $\mathbf{A^{Py}}$ was synthesized through Sonogashira coupling of a pyrene unit at the 8-position of a 2′-deoxyadenosine base.[6] We used standard phosphoramidite methods and a DNA synthesizer to incorporate pyrene-labeled deoxyadenosine building blocks into the oligodeoxynucleotides (ODNs) given in Figure 1.[7]

Figure 2A displays the steady-state absorption and fluorescence spectra of the ODN **A1**, which possesses one $\mathbf{A^{Py}}$. These spectra are quite different from those of 1-ethynylpyrene (inset) and unmodified pyrene, both of which exhibit absorption in the UV region and fluorescence at 370−430 nm with relatively sharp vibronic structures.[5] In comparison, the absorption and fluorescence signals of the single-stranded oligodeoxyadenylate **A1** were significantly red-shifted, and exhibited a broad and

(1) (a) Saenger, W. *Principles of Nucleic Acid Structure*; Springer: New York, 1984. (b) Henry, A. A.; Romesberg, F. E. *Curr. Opin. Chem. Biol.* **2003**, *7*, 727. (c) Brotschi, C.; Leumann, C. J. *Angew. Chem.. Int. Ed.* **2003**, *42*, 1655. (d) Beuck, C.; Singh, I.; Bhattacharya, A.; Hecker, W.; Parmar, V. S.; Seitz, O.; Weinhold, E. *Angew. Chem., Int. Ed.* **2003**, *42*, 3958. (e) Kool, E. T. *Acc. Chem. Res.* **2002**, *35*, 936. (f) Guckian, K. M.; Schweitzer, B. A.; Ren, J.; Rex, X.-F.; Sheils, C. J.; Tahmassebi, D. C.; Kool. E. T. *J. Am. Chem. Soc.* **2000**, *122*, 2213.

(2) (a) Ren, J.; Chaires, J. B. *Biochemistry* **1999**, *38*, 16067. (b) Wolfe, A.; Shimer, G. H.; Meehan, T. *Biochemistry* **1987**, *26*, 6392.

(3) (a) Kool, E. T.; Morales, J. C.; Guckian, K. M. *Angew. Chem., Int. Ed.* **2000**, *39*, 990. (b) Baruah, H.; Day, C. S.; Wright, M. W.; Bierbach, U. *J. Am. Chem. Soc.* **2004**, *126*, 4492. (c) Sandström, K.; Wärmländer, S.; Bergman, J.; Engqvist, R.; Leijon, M.; Gräslund, A. *J. Mol. Recognit.* **2004**, *17*, 277.

(4) (a) Wang, X.; Nau, W. M. *J. Am. Chem. Soc.* **2004**, *126*, 808. (b) Chan, S.; Nelson, J. H. *J. Am. Chem. Soc.* **1969**, *91*, 168. (c) Jain, S. S.; Polak, M.; Hud, N. V. *Nucleic Acids Res.* **2003**, *31*, 4608. (d) Persil, Ö.; Santai, C. T.; Jain, S. S.; Hud, N. V. *J. Am. Chem. Soc.* **2004**, *126*, 8644.

(5) (a) Jones, G.; Vullev, V. I., II. *J. Phys. Chem. A* **2001**, *105*, 6402. (b) Winnik, F. M. *Chem. Rev.* **1993**, *93*, 587.

(6) (a) Sonogashira, K.; Tohda, Y.; Hagihara, N. *Tetrahedron Lett.* **1975**, 4467. (b) Hwang, G. T.; Son, H. S.; Ku, J. K.; Kim, B. H. *Org. Lett.* **2001**, *3*, 2469. (c) Hwang, G. T.; Son, H. S.; Ku, J. K.; Kim, B. H. *J. Am. Chem. Soc.* **2003**, *125*, 11241. (d) Hwang, G. T.; Seo, Y. J.; Kim, B. H. *J. Am. Chem. Soc.* **2004**, *126*, 6528. (e) Seo, Y. J.; Kim, B. H. *Chem. Commun.* **2006**, *150*. (f) Seo, Y. J.; Ryu, J. H.; Kim, B. H. *Org. Lett.* **2005**, *7*, 4931. (g) Mayer, E.; Valis, L.; Wagner, C.; Rist, M.; Amann, N.; Wagenknecht, H. A. *ChemBioChem.* **2004**, *5*, 865.

(7) (a) Gait, M. J. *Oligonucleotide Synthesis: A Practical Approach;* IRL Press: Washington, DC, 1984. (b) Hwang, G. T.; Seo, Y. J.; Kim, B. H. *Tetrahedron Lett.* **2005**, *46*, 1475. (c) Seo, Y. J.; Hwang, G. T.; Kim, B. H. *Tetrahedron Lett.* **2006**, *47*, 4037. (d) Venkatsan, N.; Seo, Y. J.; Bang, E. K.; Park, S. M.; Lee, Y. S.; Kim, B. H. *Bull. Korean Chem. Soc.* **2006**, *27*, 613. (e) Seo, Y. J.; Jeong, H. S.; Bang, E. K.; Hwang, G. T.; Jung, J. H.; Jang S. K.; B. H. Kim. *Bioconjugate Chem.* **2006**, *17*, 1151.

10.1021/ja069069i CCC: $37.00

A1 5'd-AAAA^{Py}AAAAAAAAAAAAATT
A2 5'd-AAAA^{Py}A^{Py}AAAAAAAAAAAATT
A3 5'd-AAAA^{Py}AA^{Py}AAAAAAAAAAATT
A4 5'd-AAAA^{Py}AAA^{Py}AAAAAAAAAATT
A5 5'd-AAAA^{Py}AAA^{Py}AAA^{Py}AAA^{Py}AAAAATT
A6 5'd-GTGCCGAAAA^{Py}AAA^{Py}AAA^{Py}AAA^{Py}AACTGCGC
A7 3'd-CACGGCAAAA^{Py}AAA^{Py}AAA^{Py}AAA^{Py}AAGACGCG
A8 5'd-AAAAAAAAAAAAAAAAAATT
A9 3'd-TTTTTTTTTTTTTTTTTAA
A10 5'd-GTGCCGAAAAAAAAAAAAAACTGCGC
A11 3'd-CACGGCAAAAAAAAAAAAAAGACGCG
A12 5'd-AAAA^{Py}AAAA^{Py}AAAAAAAAAATT
A13 5'd-AAAA^{Py}AAAAA^{Py}AAAAAAAAATT
A14 5'd-AAAA^{Py}AAAAAA^{Py}AAAAAAAATT

Figure 1. Designed oligonucleotide sequences.

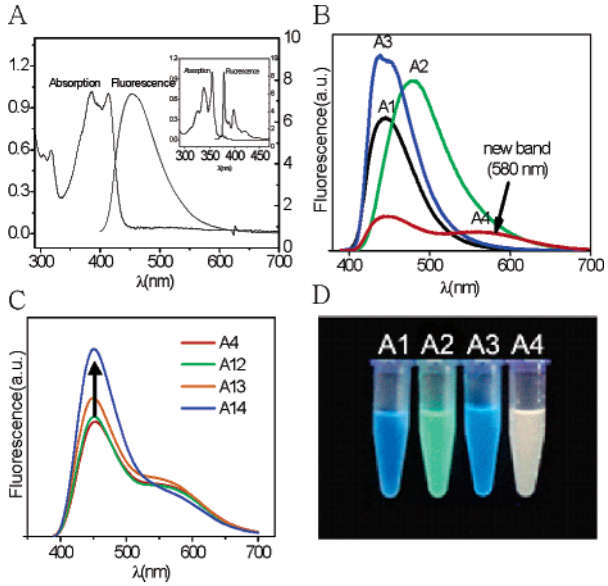

Figure 2. (A) Steady-state absorption and fluorescence spectra for **A1**. The inset shows the absorption and fluorescence spectra of ethynylpyrene. (B) Fluorescence spectra of **A1**−**A4**, recorded at λ_{ex} = 386 nm. (C) Fluorescence spectra of **A4**, **A12**−**A14**, which differ in their position of A^{Py} units. (D) Photographic image displaying the fluorescence of **A1**−**A4**, which are single oligodeoxyadenylate strands incorporating A^{Py} units. Spectra were recorded at 20 °C in a buffer of 100 mM Tris-HCl, 10 mM $MgCl_2$, and 100 mM NaCl (pH 7.2). Each concentration was 1.5 μM.

featureless band at 443 nm, quite different from those of pyrene and the ethynyl pyrene monomer.

When a second A^{Py} fluorophore was positioned adjacent to the first A^{Py} unit (i.e., in **A2**), the fluorescence signal shifted to 478 nm, that is, **A2** displays a green signal. In contrast, when these two A^{Py} units were separated by an unsubstituted adenosine (i.e., in a 1,3 relationship in **A3**), the signal returned to 439 nm and the spectrum resembles that of monosubstituted **A1**. Surprisingly, when the two A^{Py} units were positioned in a 1,4 relationship (i.e., in **A4**), a new band appeared at λ_{max} = 580 nm (reddish fluorescence) (Figure 2B), one that is not observed for pyrene itself (pyrene exhibits blue and green fluorescence for its monomer and excimer, respectively).

Only oligomers that possess more than two spacer units between the pyrene chromophores exhibit such a reddish band at 580 nm. The intensity of the band at 580 nm slowly decreased upon increasing the distance between the two A^{Py} units, but it did not disappear completely (Figure 2C). Figure 2D indicates

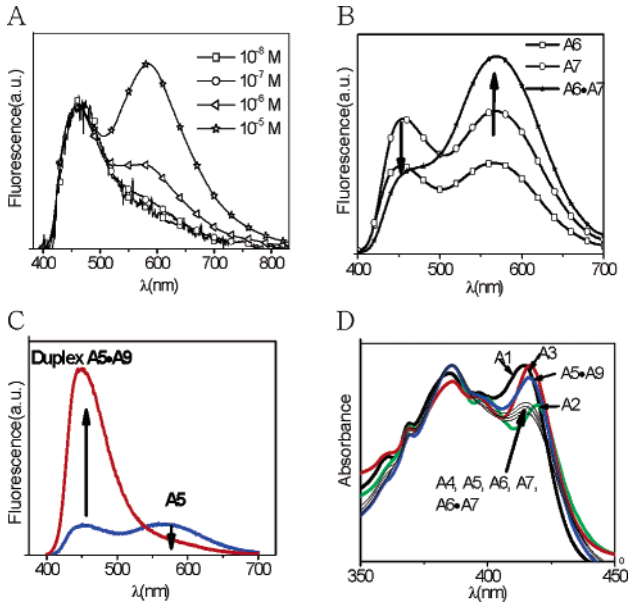

Figure 3. (A) Effect of concentration on the fluorescence of **A4**; (B) fluorescence spectra of **A6**, **A7**, and **A6·A7**; (C) fluorescence spectra of the single-stranded oligodeoxyadenylate **A5** and its duplex with complementary sequence **A9**; (D) UV absorption data for ODNs, recorded at 20 °C in 10 mM Tris-HCl (pH 7.2), 100 mM NaCl, 20 mM $MgCl_2$ (1.5 μM).

that these different signals were clearly distinguishable by the naked eye. These changes in λ_{max} mean that an oligodeoxyadenylate chain possessing two A^{Py} units displays one of three different colors (reddish-orange, green, or blue) depending upon the relative location of its fluorophore pair. Upon increasing the number of A^{Py} units on the same 1,4 relationship (i.e., in ODN **A5**), the intensity of the red fluorescence for ODN **A5** was enhanced relative to that of **A4** (Figure S1). From these results, we surmise that the appearance of this new band is related to the distance between the pairs of A^{Py} units and to the number of such pairs.

We investigated whether other sequences can lead to systems that act as three-color platforms. For sequence studies, we incorporated the two A^{Py} into the corresponding oligodeoxythymidylate, oligodeoxyguanosylate, and oligodeoxycytidylate; interestingly, we did not observe oligodeoxyadenylate-like phenomena in these systems (see Supporting Information). Therefore, we believe that the band at 580 nm is a unique characteristic of the conformations of the oligodeoxyadenylates, which may be related to the unique electronic properties of their conformations; distinct stacking properties and rigidity of single-stranded oligodeoxyadenylates are well-known.[4]

To deduce the origin of this new spectral feature, that is, to determine whether it arose from the intramolecular or intermolecular interactions, we recorded the fluorescence spectra of **A4** at various concentrations (Figure 3A). Decreasing the concentration caused a reduction in the intensity of the red-shifted band. The concentration dependence of the signals in these spectra suggests that the interaction leading to the appearance of the reddish band is intermolecular in origin.

We synthesized the base sequences of ODNs **A6** and **A7** (derivatives of **A5** that possess complementary termini) to induce the intermolecular interaction artificially. From the fluorescence spectra in Figure 3B, we observed that the duplex **A6·A7** reveals a significantly increased reddish band intensity, while **A6** and **A7** exhibit relatively weak reddish bands. We also synthesized

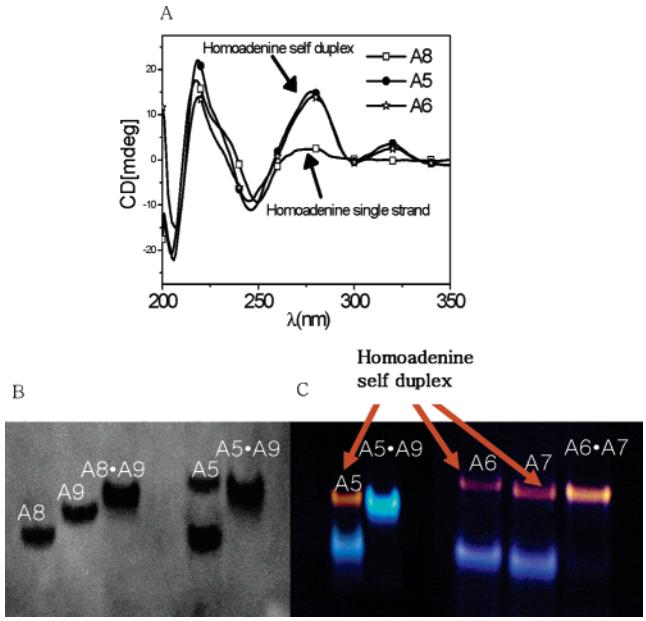

Figure 4. (A) CD spectra of ODNs **A8**, **A5**, and **A6**; (B and C) gel electropherograms indicate the self-duplex structures of the pyrene-substituted oligodeoxyadenylates; (B) image obtained after staining; (C) image obtained when using a UV analyzer (without staining). See the Experimental Section for details of the sample preparation procedure.

the complementary sequence ODN **A9** to ODN **A5** to inhibit the intermolecular interaction (of ODN **A5**). After adding ODN **A9**, the fluorescent reddish band at 580 nm of ODN **A5** disappeared and the blue-shifted band increased (Figure 3C), which is well consistent with absorption spectra at 420 nm (characteristic band of pyrene monomer): the absorption band is increased after forming the duplex **A5·A9** (Figure 3D). These experiments confirm that the reddish band originates from the intermolecular interaction.

In absorption spectra, the ODNs **A4**, **A5**, **A6**, **A7** and duplex **A6·A7** show the same absorption spectra patterns (corresponding to the pyrene region), while, the ODNs **A1**, **A2**, and **A3** show the different absorption band patterns as shown in Figure 3D. The decrease in intensity of the absorption band at 420 nm, in ODNs **A4**, **A5**, **A6**, **A7** and the duplex **A6·A7**, explain the intermolecular interaction of pyrenes in these ODNs.[1f,6e−g]

The CD data show a further interesting result. The natural oligodeoxyadenylate ODN **A8** and the pyrene-modified systems ODN **A5** and ODN **A6** present different band patterns; whereas ODN **A8** displayed a single-stranded character, surprisingly, the pyrene-modified ODNs **A5** and **A6** both exhibited the characteristics of duplexes (Figure 4A). The band pattern of ODNs **A5** and **A6** was similar to the CD data for a homoadenine self-duplex reported by Hud and co-workers.[4d] We could see the duplex formation in the AFM image (the height is 1 nm, which is the duplex height) (Figure S6).

To confirm that self-duplex formation, we measured the migrations of ODNs **A5**−**A9** on a nondenaturing polyacrylamide gel (Figure 4B,C). As expected, natural ODN **A8** exhibited the mobility of a single strand (Figure 4B), while modified ODNs **A5**, **A6**, and **A7** exhibited both duplex and single-strand mobility with clear indication of homoadenine self-duplex formation. Interestingly, from direct visual examination of the gel, we observed that the reddish fluorescence was emitted in the region of duplex mobility of the ODNs **A5**, **A6**, and **A7** (Figure 4C).

Table 1. Time-Resolved Fluorescence Time Constants Obtained from TCSPC Data for Oligomers **A1**−**A4**

	A1	A2	A3	A4
τ^a (ns)	2.6	3.4	4.1	2.8
τ^b (ns)	2.6	3.3 (0.53)[c] 33 (0.47)	4.5	42

[a] Fitted time constants probed on the blue side (440 nm) of the fluorescence spectrum, corresponding to the monomer band. [b] Fitted time constants probed on the red edges (**A1**, 620 nm; **A2**, 640 nm; **A3**, 580 nm; **A4**, 660 nm) of the fluorescence spectrum, corresponding to the interaction band. [c] Values in parentheses are the relative amplitudes obtained from a double-exponential fit.

For the **A6·A7** duplex, the artificially induced self-duplex of oligodeoxyadenylate, most of the signals show a strong reddish band intensity in the region of duplex mobility, which means the structure origin of the reddish band at 580 nm is an intermolecular self-duplex of olygodeoxyadenylate.

The melting temperatures of these ODNs (Figure S7) provided further information supporting the formation of self-duplexes. The melting temperature (67 °C) of ODN **A6·A7** (a pyrene modified duplex) was much higher than that (44 °C) of ODN **A10·A11** (an unmodified duplex of ODN **A6·A7**). This increase in melting temperature (23 °C) must come from the pyrene intercalation in the self-duplex of the oligodeoxyadenylate region of ODN **A6·A7**. Although the melting curves of ODNs **A6** and **A7** were broad, their melting temperatures were observed in the region from ∼48 to 56 °C, suggesting the formation of the homoadenine self-duplexes.

Next, we performed time-resolved fluorescence measurements of the ODNs **A1**−**A4** using the time-correlated single-photon counting (TCSPC) and upconversion methods in an effort to examine the properties of the reddish band. Table 1 presents the picosecond time-resolved fluorescence of ODNs **A1**−**A4** as measured by TCSPC while monitoring the fluorescence at 440 and 580−660 nm, that is, at wavelengths that correspond to the monomer and red-shifted bands, respectively.

The data were fit by exponential functions and Table 1 gives the time constants. For **A1** and **A3**, fluorescence time profiles do not depend on the detection wavelength indicating that the fluorescence is due to the pyrene monomer exclusively. In **A2** and **A4** (and **A*n***, $n > 4$), however, the time profiles are distinctively different from that of **A1**. When measured at the monomer (**A1**) emission maximum, the time constants are similar to that of the monomer, whereas they are much longer (∼10 times) at the red band. Moreover, time-resolved fluorescence for all samples measured at the red band (**A2**, 640 nm; **A4**, 660 nm) show instrument-limited rise even at the time resolution of 100 fs (data not shown). This clearly indicates that the red-shifted bands in **A2** and **A4** do not originate from the excimer formation. Excluding the possibility of excimer formation, on the basis of the results of our time-resolved fluorescence experiment, we propose the following explanation for the phenomena. In both **A2** and **A4**, pyrenes form an interacting pair in the ground state, and *J*-type exciton couplings lead to the red-shifted bands. The amount of red-shifts and the lifetimes of the red band in **A2** and **A4**, however, are different to denote distinct interaction geometries. Adjacent pyrenes units in **A2** should interact naturally because of the proximity, while the pyrenes in **A4** interacts intermolecularly to form two pyrene dimers in the ground state, which give a much more red-shifted

emisison band. This conclusion is consistent with the absorption spectra, gel electrophoresis, and CD data.

In conclusion, we have observed that homoadenine self-duplexes can form when pyrene units are covalently bound to bases positioned at specific distances (1,4 relationships). These duplexes feature a unique fluorescence signal, a red band peaking at 580 nm, and the life time of this band is long (42 nanoseconds). The results of several spectroscopic experiments suggest that the unique signal at 580 nm arises mainly from intermolecular self-duplex formation between the $\mathbf{A^{Py}}$-substituted oligodeoxyadenylates. This serendipitous discovery provides an excellent illustration of how small-molecule binding can be induced to alter nucleic acid secondary structure with a concomitant change in the fluorescence signal. We believe that this system provides the first example of nonpolar, hydrophobic, planar units inducing self-duplex formation of oligodeoxyadenylates, with a new reddish band appearing at 580 nm. This interesting discovery suggests that the small intercalators triggering the formation of non-Watson−Crick secondary structures would be useful in the design of dynamic DNA nanostructures and new biosensor systems. We are studying the ability of such ODNs containing $\mathbf{A^{Py}}$ units to probe the biomolecule (structure) such as protein, DNA, by making use of the unique reddish pyrene fluorescence as a new signal system.

Experimental Section

Time-Resolved Fluorescence (TRF). A cavity-dumped Kerr lens mode-locked Ti:sapphire laser generating 20 fs pulses was used as a light source. The center wavelength was 770 nm, the repetition rate was 380 kHz, and the energy per pulse was 65 nJ. Two methods were used to measure the time-resolved fluorescence over different time-scales. The picosecond time-resolved fluorescence experiments were performed through time-correlated single-photon counting (TCSPC)[8] and employing a microchannel plate photomultiplier tube. The instrumental response was 40 ps (fwhm), allowing a time-resolution of ~8 ps after deconvolution. The subpicosecond dynamics were measured using an upconversion technique that has been described previously.[9,10] Briefly, the second harmonic (385 nm) of the fundamental (770 nm) pulse was used as a pump pulse and the residual 770 nm pulse was used as a gate pulse. The upconversion signal was obtained through noncollinear phase-matching to minimize the effect of group velocity mismatch (GVM) broadening. The time-resolution of the upconversion setup was ~100 fs (fwhm) when using a 500 μm BBO crystal.

Sample Preparation for Gel Electrophoresis. Electrophoresis of 6 μL sample with loading buffer was performed under nondenaturing conditions using a 20% polyacrylamide gel [40% acrylamide (4 mL), 5× TBE buffer (1.6 mL), $(NH_4)_2S_2O_8$ (0.1 g), *N*,*N*,*N*',*N*'-tetramethylethylenediamine (5 μL), and distilled water (2.4 mL)] and the following conditions: 135 V, 20 mA, 200 W, and 4 °C. To obtain Figure 4B, after running the gel, the gel was mixed with the nucleic acid-staining material Stains-All (Sigma) in distilled water for 30 min. The gel was dried and exposed on a Canon PowerShot A75. To obtain Figure 4C, after electrophoresis, the gel was displayed on an SL-20 high-performance DNA Image Visualizer, without using Stains-All; the photographic image was recorded using a Canon PowerShot A75. Analysis of the image was performed using Photoshop (v. 7.0) software.

Acknowledgment. We are grateful to KOSEF for financial support through the National Research Laboratory Program (Laboratory for Modified Nucleic Acid Systems), Gene Therapy R&D program (M10534000011-05N3400-01110) and KNRRC program.

Supporting Information Available: MALDI-TOF mass spectral data; fluorescence spectra of the altering number of $\mathbf{A^{Py}}$, the other oligomer, and $\mathbf{U^{Py}}$ systems; denaturing gel electropherograms; melting temperatures of ODNs; AFM image of ODNs; time-resolved fluorescence spectra of ODNs **A1**−**A4.** This material is available free of charge via the Internet at http://pubs.acs.org.

JA069069I

(8) Lee, M.; Kim, D. *J. Opt. Soc. Korea* **1990**, *1*, 52.
(9) Yoon, M.-C.; Jeong, D. H.; Cho, S.; Kim, D.; Rhee, H.; Joo, T. *J. Chem. Phys.* **2003**, *118*, 164.
(10) Rhee, H.; Joo, T. *Opt. Lett.* **2005**, *30*, 96.